Diode-pumped, narrow-linewidth, linearly polarized, passively *Q*-switched 1645 nm Er:YAG laser

Zhenzhen Yu (于真真)[1,2], Mingjian Wang (王明建)[1], Xia Hou (侯 霞)[1], and Weibiao Chen (陈卫标)[1,*]

[1]*Key Laboratory of Space Laser Communication and Detection Technology, Shanghai Institute of Optics and Fine Mechanics, Chinese Academy of Sciences, Shanghai 201800, China*

[2]*University of Chinese Academy of Sciences, Beijing 100049, China*

**Corresponding author: wbchen@siom.ac.cn*

Received March 26, 2015; accepted May 7, 2015; posted online June 22, 2015

We demonstrate a narrow-linewidth linearly polarized 1645 nm Er:YAG laser, directly diode-pumped by a fiber-coupled continuous-wave laser diode at 1532 nm. Passive *Q*-switching is realized by a few-layer graphene saturable absorber. A maximum polarized average output power of 3.13 W is achieved at 23.28 W incident pump power. A pulse energy of as much as 58.8 μJ and pulse width of 4.21 μs are yielded at a 53.2 kHz pulse repetition rate. The spectrum and linewidth of the output beams are measured to be 1645.34 and 0.05 nm, respectively. This laser can be useful in the detection of atmosphere pollutants.

OCIS codes: 140.3500, 140.3480, 140.3580, 140.3540.

doi: 10.3788/COL201513.071403.

Eye-safe *Q*-switched lasers at 1.5–1.6 μm are playing an increasingly important role in ranging, remote sensing, and free-space communications[1,2]. High-energy and high-efficiency laser sources can be obtained based on the active *Q*-switching, which, however, involves a high-voltage driver or an additional radio frequency (RF) generator. Distinct from the active *Q*-switching, the passive *Q*-switch regime allows more compact and simpler resonator designs. In the past few years, passively *Q*-switched eye-safe erbium lasers have become an active research field and have been demonstrated with Cr:ZnSe as saturable absorbers (SAs) for *Q*-switching at 1.6 μm[3,4]. Pulses with pulse width of tens of nanoseconds and pulse repetition rate of hundreds of hertzs were obtained. With respect to SAs, graphene has recently received much attention[5–7] and has proven to be a promising SA benefiting from its low-saturation intensity, high damage threshold, ultrafast recovery time, low cost, and tunable SA modulation depth[8–16]. Besides, unlike conventional SAs (Cr:ZnSe and so on), the saturable absorption range of graphene is broadband (300–2500 nm), which favors the operation of *Q*-switching or mode-locking in the aforementioned 300–2500 nm spectral range[15,16]. Passively *Q*-switched operation of 1.6 μm erbium-doped single-crystal or polycrystalline ceramic lasers have been demonstrated with graphene as SAs[10–14]. The obtained pulse width was of several microseconds and pulse repetition rate of tens of kilohertz. Gao *et al.* (2012) reported a fiber laser resonantly pumped graphene-based passively *Q*-switched Er:YAG laser at 1645 nm with 7.05 μJ single-pulse energy and 35.6 kHz pulse repetition rate[11]. Zhu *et al.* (2013) demonstrated an in-band pumped polycrystalline 1645 nm Er:YAG ceramic laser by using graphene as a SA and a fiber laser pumping source; 7.08 μJ single-pulse energy was generated at a 74.6 kHz pulse repetition rate[13]. However, the pumping approach with fiber lasers has the drawback of system complexity, reducing the benefit of the use of a SA as a *Q*-switch system. Additionally, the entire efficiency of the laser system is restricted because of the fiber laser stage, which is pumped by 976 nm laser diodes (LDs). Alternatively, directly-diode pumped erbium lasers have been developed and are more compact and simpler eye-safe sources[4,14]. Zhou *et al.* (2014) demonstrated a passively *Q*-switched 1645 nm Er:YAG laser pumped by a LD at 1532 nm. With a monolayer graphene SA, *Q*-switched pulses of 13.5 μJ pulse energy and 0.13 nm linewidth were achieved[14]. However, few studies have addressed the polarization control of the output beams, which is beneficial to the detection of atmosphere pollutants or materials[17,18].

In this Letter, we report the operation of a 1532 nm LD in-band pumped Er:YAG laser at 1645 nm, and passive *Q*-switching was performed with graphene as the SA. Linearly polarized output was achieved by using a cavity mirror with high reflection for s-polarized light at 1.6 μm. A polarized output with up to 58.8 μJ pulse energy was obtained at 53.2 kHz pulse repetition frequency, and the measured linewidth of the output 1645 nm laser was about 0.05 nm. To our knowledge, there is no report on directly diode pumped graphene *Q*-switched erbium lasers with both narrow linewidth and linear polarization.

A schematic of the diode-pumped passively *Q*-switched Er:YAG laser is depicted in Fig. 1. The L-shaped plano-concave resonator has an optical cavity length of about 120 mm for compactness reasons. A flat mirror M1 with both high-reflectivity (>99.5%) at 1.6–1.7 μm wavelength and anti-reflection (AR) (>95%) at 1532 nm was used as the rear mirror. A plano-concave mirror M3 was used as the output coupler with different transmissions of 15%

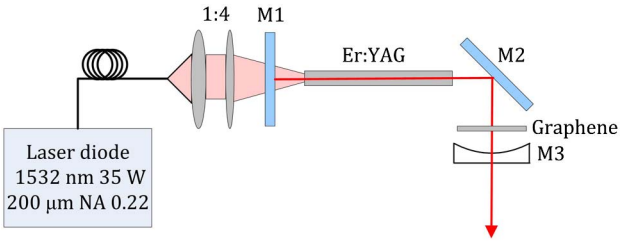

Fig. 1. Layout of Er:YAG laser with directly diode-pumping and graphene Q-switching.

and 20% at the wavelength of 1.6 μm. Its curvature was 500 mm. A few-layer graphene (Shandong University), synthesized by the chemical vapor deposition (CVD) method and covered on a 1 mm thick quartz substrate, was used to obtain passive Q-switching. It had a clear aperture of 10 mm × 10 mm. The folding mirror M2 was planar and dichroic with AR (>97.2%) at 1.5 μm pump wavelength and high-reflectivity (>99.5%) for s-polarized light at 1.6 μm (less than 70% reflectivity for the p-polarized light at 1.6 μm), which not only was useful for the linearly polarized laser output, but also avoided the thermal instability effect of the unabsorbed pumping light (about 50% of the incident pump power) on the graphene SA.

The laser medium was a 4 mm diameter, 40 mm long Er:YAG crystal with 0.25 at.% doping concentration, which can minimize reabsorption and energy transfer upconversion (ETU) at the lasing wavelength. The Er:YAG crystal were polished on the two end-surfaces and AR-coated for 1.5–1.7 μm wavelength. The damage threshold of the coatings was about 500 MW/cm^2. Wrapped with indium foil, it was placed in a water-cooled copper heat sink. The temperature of the cooling water was maintained at ~288 K in our work. The pump source was a fiber-coupled 1532 nm LD (QPC lasers) with up to 35 W output power. The core diameter and numerical aperture of the fiber was 200 μm and 0.22, respectively. Its spectral width was narrowed to about 1 nm by internal Bragg gratings. By using the ABCD matrix method and with the thermal lens effect of the Er:YAG crystal considered, a calculated diameter of the laser transverse electric and magnetic field $(TEM)_{00}$ mode was about 674 μm on the graphene SA and 660 μm in the middle of the crystal. The laser beam diameters were believed to have little difference in continuous-wave (CW) and Q-switched modes since the graphene SA was thin and had insignificant thermal effects. The pump light of the LD was focused by a 1:4 coupling system to a few millimeters inside the Er:YAG crystal with a radius of less than 400 μm. To protect optical components from damage at higher incident diode pump powers, the intracavity peak-power density was kept no more than 500 MW/cm^2 by using an output coupler with high transmission, designing a large-radius TEM_{00} mode, and limiting the maximum incident pump power.

The performance of the Er:YAG laser in CW operation was first studied with a 15% transmission output coupler. A 7.42 W CW output power was achieved as the incident pump power was 24.75 W, and the corresponding optical conversion efficiency was 30%. When a 20% transmission output coupler was employed, the output power was lowered to 5.47 W with 22.1% optical conversion efficiency. For passive Q-switching, the few-layer graphene was placed inside the laser cavity. Although the output coupler with 15% transmission exhibited better laser performance, the 20% transmittance output mirror was adopted to avoid optical damage of the graphene, and at the same time the maximum incident pump power was lowered to 23.5 W. At 23.28 W incident pump power, a maximum average output power of 3.13 W was yielded with 13.4% optical conversion efficiency. Compared with the performance in the CW mode, the output power and the optical conversion efficiency were reduced, which was caused by the increased intracavity loss induced by the uncoated graphene on quartz and the absorption of graphene.

The input-output characteristics of the Er:YAG laser in the CW and passively Q-switched regime is shown in Fig. 2. The quasi-linear feature of the output power curves was caused by the pump wavelength shifting as the pump power increased (from 1531.08 nm at 17.85 W to 1532.37 nm at 25 W) in spite of the internal grating, and similar effects have already been noticed in Refs. [4,19]. The polarization of the output beam was measured by the combination of a half-wave plate and a polarizer. By rotating the half-wave plate and measuring the laser power through the polarizer, the polarization extinction ratio of the output beam was larger than 20 dB.

The spectrum of the Er:YAG laser was measured with a spectrograph (AQ6370B, Yokogawa). Figure 3 illustrates the laser spectrum in the CW and passively Q-switched mode of the Er:YAG laser at 23.28 W incident pump power. For the CW operation, It can be seen that a multiline mode was obtained. For the passive Q-switching,

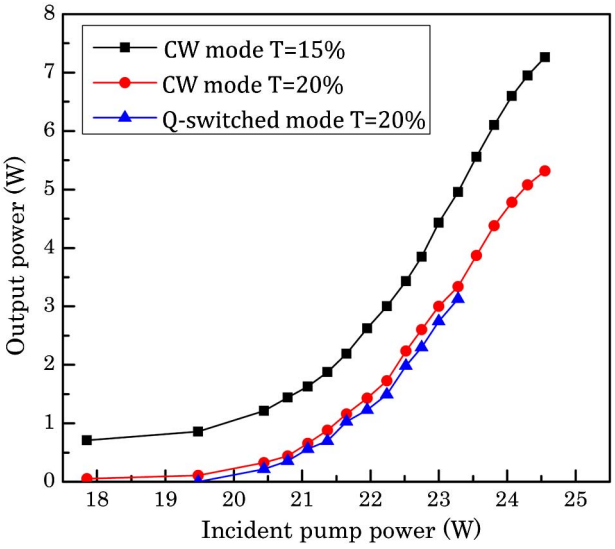

Fig. 2. Input–output characteristics in CW and Q-switched mode.

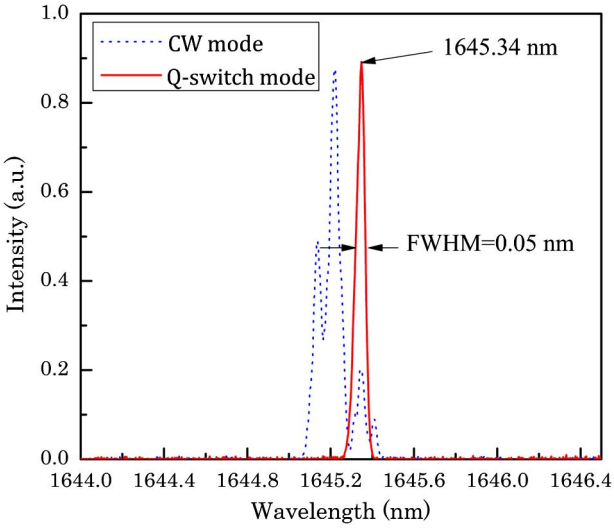

Fig. 3. Measured spectrum of the Er:YAG laser. Dashed line, spectrum in CW mode.

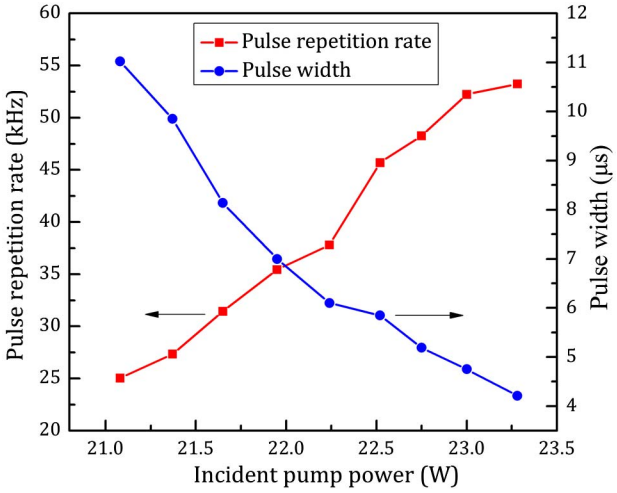

Fig. 5. Relationship between pulse repetition rate or pulse width and incident pump power.

the laser spectrum was centered at 1645.34 nm with a spectral width of ~0.05 nm. One primary reason for the narrowed spectrum in Q-switch mode is that the SA component can action as an equivalent Fabry–Perot (F–P) etalon[14]. In addition, it takes a long build-up time for the oscillation pulses in passive Q-switching[3], which could also result in narrowing of the spectral width. Therefore, narrow linewidth of the oscillation can be achieved without the use of an intracavity spectral selector.

The temporal profile of output pulses was recorded by an InGaAs detector (DET01CFC, Thorlabs) and is depicted in Fig. 4. The pulse repetition rate and pulse width were measured to be 53.2 kHz and 4.21 μs, respectively, at 3.13 W maximum average output power. The standard deviations of the pulse repetition rate and pulse width are 0.48 kHz and 0.23 μs. The intensity fluctuation among pulses was estimated to be less than 10%. Figure 5 shows the relationship between the pulse repetition rate or pulse width and the incident pump power. With increasing incident pump power, the pulse repetition rate went up from 28.6 to 53.2 kHz, while the pulse width decreased from 10.77 to 4.21 μs. Based on Refs. [9,13], a shorter pulse duration can be obtained by reducing the layer number of graphene. Future work will focus on the optimization of the layer number of graphene and resonator parameters.

Figure 6 shows the connection between single pulse energy and incident pump power. Up to 58.8 μJ single-pulse energy was achieved at an incident pump power of 23.28 W. Besides, under a maximum optical fluency of about 155 mJ/cm^2, there was no obvious damage on the graphene SA. The beam profiles were measured by using an InGaAs camera and a plano-convex lens at the maximum output pulse energy. The beam quality parameters were calculated from these images with the second momentum technique, as described in the ISO11146 norm. Figure 7 shows the beam profiles and beam quality parameters ($M_X^2 = 1.46$ and $M_Y^2 = 1.35$). The slightly elliptical beam profiles were the result of asymmetrical heat dissipation of the rod, as well as the tilted mirror M2, which added some astigmatism to the beam profile.

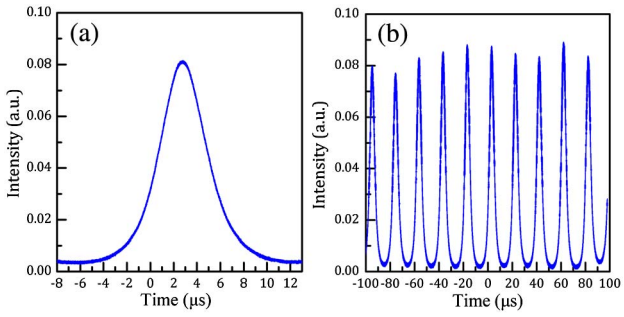

Fig. 4. Pulse shape at 53.2 kHz pulse repetition rate: (a) single-pulse and (b) pulse train.

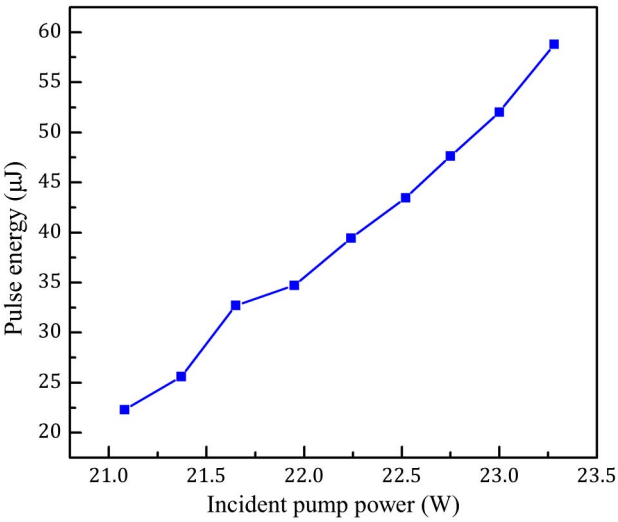

Fig. 6. Relationship between pulse energy and incident pump power.

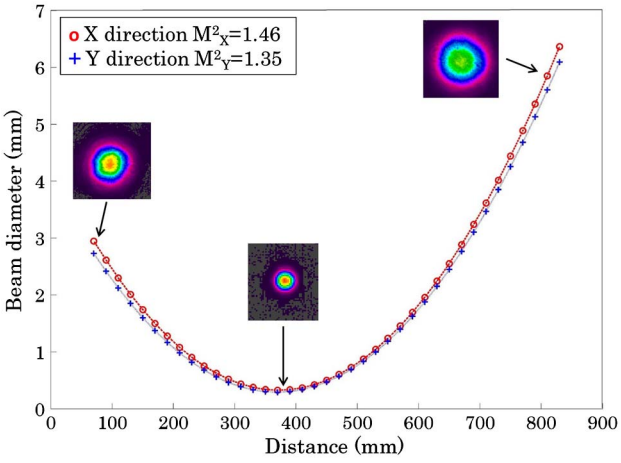

Fig. 7. Beam characterization at the maximum average output power.

In conclusion, we demonstrate a passively Q-switched 1645 nm Er:YAG laser directly diode-pumped by a CW fiber-coupled LD at 1532 nm. Laser beams with linear polarization and linewidth of about 0.05 nm are achieved with a precise experimental setup. With a few-layer graphene as the SA, pulses with up to 58.8 μJ pulse energy, 53.2 kHz pulse repetition rate, and 4.21 μs pulse width are obtained. This work can be useful for laser sources in the detection of atmospheric pollutants.

This work was supported by the National Natural Science Foundation of China under Grant No. 61405213.

References

1. R. C. Stoneman, R. Hartman, A. I. R. Malm, and P. Gatt, Proc. SPIE **5791**, 167 (2005).
2. R. C. Stoneman, R. Hartman, E. A. Schneider, C. G. Garvin, and S. W. Henderson, Proc. SPIE **6552**, 65520H (2007).
3. I. S. Moskalev, V. V. Fedorov, V. P. Gapontsev, D. V. Gapontsev, N. S. Platonov, and S. B. Mirov, Opt. Express **16**, 19427 (2008).
4. A. Aubourg, J. Didierjean, N. Aubry, F. Balembois, and P. Georges, Opt. Lett. **38**, 938 (2013).
5. S. Han, X. Li, H. Xu, Y. Zhao, H. Yu, H. Zhang, Y. Wu, Z. Wang, X. Hao, and X. Xu, Chin. Opt. Lett. **12**, 011401 (2014).
6. R. Z. R. R. Rosdin, F. Ahmad, N. M. Ali, S. W. Harun, and H. Arof, Chin. Opt. Lett. **12**, 091404 (2014).
7. H. Ahmad, F. D. Muhammad, M. Z. Zulkifli, and S. W. Harun, Chin. Opt. Lett. **11**, 071401 (2013).
8. H. H. Yu, X. F. Chen, H. J. Zhang, X. G. Xu, X. B. Hu, Z. P. Wang, J. Y. Wang, S. D. Zhuang, and M. H. Jiang, ASC Nano **4**, 7582 (2010).
9. Q. L. Bao, H. Zhang, Y. Wang, Z. H. Ni, Z. X. Shen, K. P. Loh, and D. Y. Tang, Adv. Funct. Mater. **19**, 3077 (2009).
10. X. F. Yang, Y. Wang, H. T. Huang, D. Y. Shen, D. Y. Tang, H. Y. Zhu, D. X. Xu, D. H. Zhou, and J. Xu, Laser Phys. Lett. **10**, 105810 (2013).
11. C. Gao, R. Wang, L. Zhu, M. Gao, Q. Wang, Z. Zhang, Z. Wei, J. Lin, and L. Guo, Opt. Lett. **37**, 632 (2012).
12. X. Zhang, J. Liu, D. Shen, X. Yang, D. Tang, and D. Fan, IEEE Photon. Technol. Lett. **25**, 1294 (2013).
13. Z. X. Zhu, Y. Wang, H. Chen, H. T. Huang, D. Y. Shen, J. Zhang, and D. Y. Tang, Laser Phys. Lett. **10**, 055801 (2013).
14. R. Zhou, P. Tang, Y. Chen, S. Chen, C. Zhao, H. Zhang, and S. Wen, Appl. Opt. **53**, 254 (2014).
15. G. Q. Xie, J. Ma, P. Lv, W. L. Gao, P. Yuan, L. J. Qian, H. H. Yu, H. J. Zhang, J. Y. Wang, and D. Y. Tang, Opt. Mater. Express **2**, 878 (2012).
16. D. Popa, Z. Sun, T. Hasan, F. Torrisi, F. Wang, and A. C. Ferrari, Appl. Phys. Lett. **98**, 073106 (2011).
17. Y. Y. Hassebo, B. Gross, M. Oo, F. Moshary, and S. Ahmed, Appl. Opt. **45**, 5521 (2006).
18. A. Aubourg, M. Rumpel, J. Didierjean, N. Aubry, T. Graf, F. Balembois, P. Georges, and M. A. Ahmed, Opt. Lett. **39**, 466 (2014).
19. M. J. Wang, L. Zhu, W. B. Chen, and D. Y. Fan, Opt. Lett. **37**, 3732 (2012).